CONTACT STRENGTH OF CERAMICS UNDER OPPOSED ROLLER LOADING

T. Fett, D. Munz, G. Thun

Forschungszentrum Karlsruhe, Institut für Materialforschung II, 76021 Karlsruhe.

Abstract: *Rectangular bars loaded by opposite concentrated forces via rollers are appropriate test specimens for the determination of strength under contact loading which comprises multiaxial stresses with very strong stress gradients. In the paper, the stress solution in the whole specimen is given for the case of a Hertzian contact stress under the loading cylinders. The contact strengths measured on several ceramics revealed significantly reduced Weibull exponents compared with those obtained from 4-point bending tests.*

1 INTRODUCTION

Conventional strength tests describe the failure behaviour of materials under simple stress conditions which, in most cases, comprise uniaxial stresses with relatively low stress gradients. In practical applications, mechanical loading often leads to strongly non-homogeneous and multiaxial stresses. For instance, this applies to contact loading by line or point loads. Predictions of strength under contact loading are possible, in principle, on the basis of the Weibull theory plus a multiaxial failure criterion. If this criterion is known for a specific ceramic, the failure probability in multiaxial and inhomogeneous stress fields can be computed by introducing into the Weibull formalism so-called effective volumes (or surfaces). This approach is applicable, at least, in cases where the stress variations are small and sufficiently constant stresses can be assumed to exist over the size of natural flaws.

In order to obtain a direct measure of failure under contact loading, a "contact strength" test was proposed in [1], as illustrated in Fig. 1. Two cylinders made of hardened steel are pressed onto the rectangular specimen with a force P. The cylinders are about 0.1 mm smaller than the guiding groove in the support structure in order to avoid any clamping during load application (cylinders become oval under load).

2 STRESSES

For the Hertzian contact between the cylinders and the plane bar, the pressure distribution acting over the region $-s \le x \le s$ is

$$p(x) = p_0 \sqrt{1-(x/s)^2}\ , \quad p_0 = \frac{2P}{s\pi\, t} \tag{1}$$

with the maximum pressure, p_0, and the contact range, $2s$, as shown in Fig. 1.

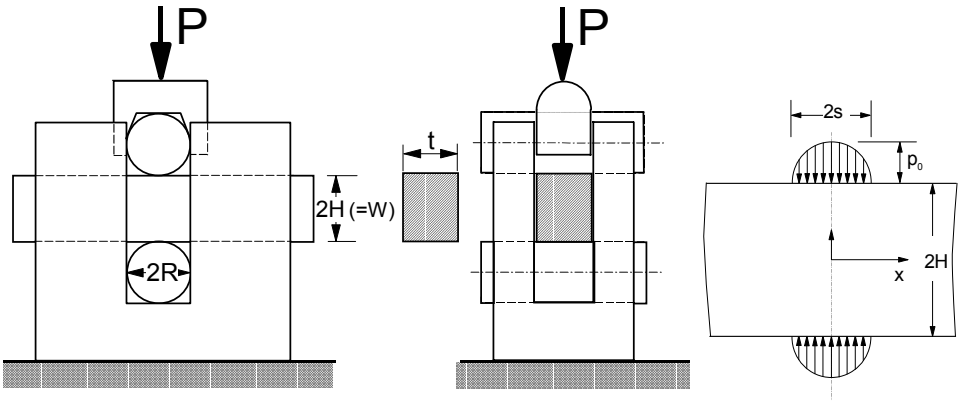

Fig. 1 A two-roller test device for contact strength tests and Hertzian pressure distribution.

Under this load, the stress components, σ_x and τ_{xy}, are

$$\sigma_x = -2p_0 \int_0^\infty \frac{1}{u} \frac{\sinh u - u\cosh u}{\sinh 2u + 2u} \cos\frac{ux}{H}\ J_1(u\,s/H) \cosh\frac{uy}{H} \mathrm{d}u$$
$$-2p_0 \int_0^\infty \frac{y}{H} \frac{\sinh u}{\sinh 2u + 2u} \cos\frac{ux}{H}\ J_1(u\,s/H)\ \sinh\frac{uy}{H} \mathrm{d}u \qquad (2)$$

$$\sigma_y = -2p_0 \int_0^\infty \frac{1}{u} \frac{\sinh u + u\cosh u}{\sinh 2u + 2u}\ \cos\frac{ux}{H} J_1(u\,s/H) \cosh\frac{uy}{H} \mathrm{d}u$$
$$+2p_0 \int_0^\infty \frac{y}{H} \frac{\sinh u}{\sinh 2u + 2u} \cos\frac{ux}{H}\ J_1(u\,s/H)\ \sinh\frac{uy}{H} \mathrm{d}u \qquad (3)$$

$$\tau_{xy} = 2p_0 \int_0^\infty \frac{1}{u} \frac{u\cosh u}{\sinh 2u + 2u}\ \sin\frac{ux}{H}\ J_1(u\,s/H)\ \sinh\frac{uy}{H} \mathrm{d}u$$
$$-2p_0 \int_0^\infty \frac{y}{H} \frac{\sinh u}{\sinh 2u + 2u} \sin\frac{ux}{H} J_1(u\,s/H)\ \cosh\frac{uy}{H} \mathrm{d}u \qquad (4)$$

with the first-order Bessel function J_1.

Maximum tensile stress in the bar is reached at the upper and lower surfaces, $y = \pm H$, directly near the rollers, ($x \approx 0$). At these locations,

$$\sigma_{\max} = 0.490\,\sigma^*, \quad \sigma^* = \frac{P}{Ht} \qquad (5)$$

In the contact strength tests, this maximum stress value was identified as the strength.

The stresses are plotted in Fig. 2, normalized to σ*. The stress component, σ_x, is represented in Fig. 2a. Tensile stresses occur close to the surface, which change to compression and back to tension in the specimen centre. The shear stresses, τ_{xy}, plotted in Fig. 2b are antisymmetric with respect to the centre line, ($y = 0$). The shorter the distance from the contact area, the steeper the stress gradients.

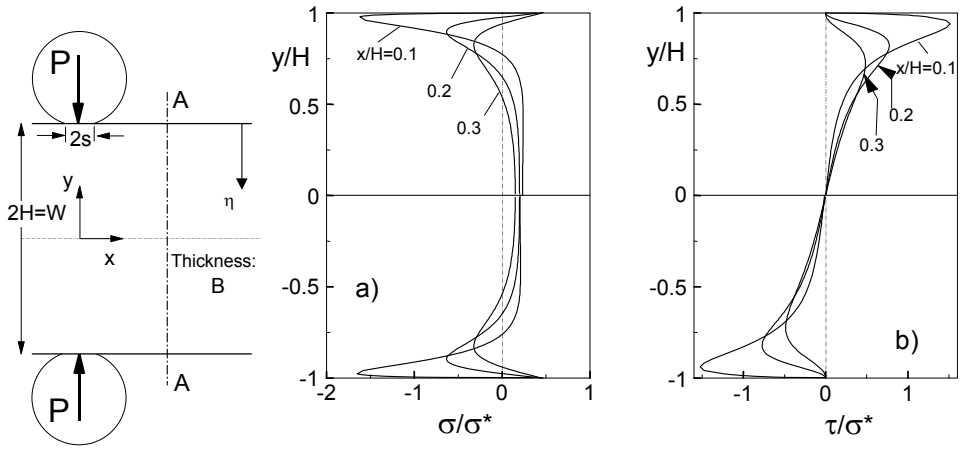

Fig. 2 Stresses for a bar loaded by a pair of opposed forces. Pure line load, $s = 0$: (a) normal stress component, σ_x, (b) shear stress, τ_{xy},

3 EXPERIMENTAL RESULTS

Contact strength tests were performed on two types of commercial aluminum oxides, coarse-grained Al_2O_3 (Frialit F99.7) and fine-grained Al_2O_3 (Frialit F99.9) both from Friatec, Friedrichsfeld.

For comparison, 4-point bending tests were carried out in addition. The strength data measured for the two aluminas are represented in Fig. 3. According to the relation for the failure probability, F,

$$F = 1 - \exp[-(\sigma_c / \sigma_0)^m] \tag{6}$$

the Weibull parameters, m and σ_0, were determined by the "Maximum Likelihood Procedure" according to [2]. The 90% confidence intervals were computed as suggested in [3].

In Fig. 4a, the 90% confidence intervals of the bending strengths are plotted versus the 90% confidence intervals of the contact strengths, including results obtained earlier [1]. The dash-dotted line suggests a linear interdependency of the two strengths. Figure 4b shows the 90% confidence intervals of the Weibull exponents for roller loading and for the bending test. The dashed line is described by

$$m_{contact} \approx \tfrac{1}{2} m_{bend} \tag{7}$$

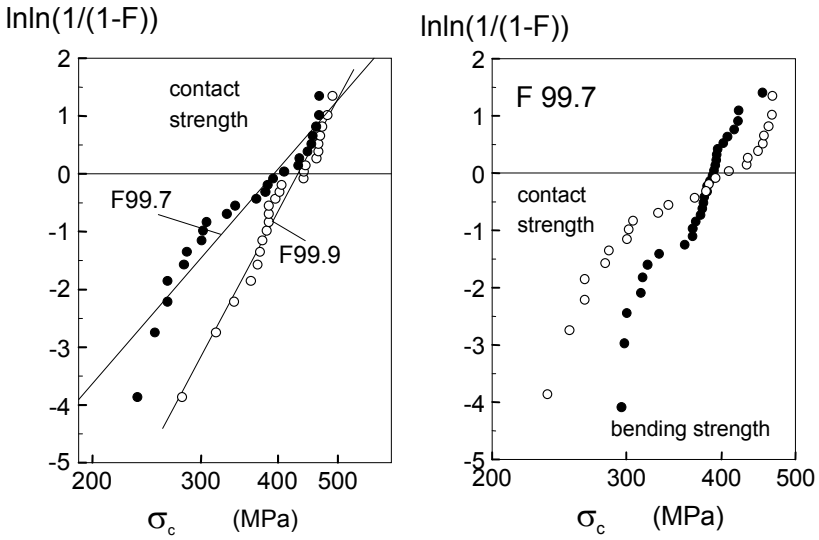

Fig. 3 Contact strengths of the alumina ceramics compared to 4-point bending strengths, from [4].

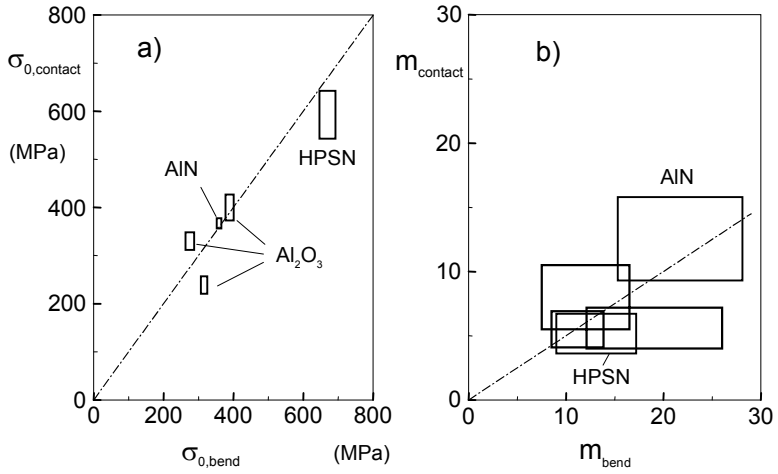

Fig. 4 Interrelation between Weibull parameters of contact strength and 4-point bending strength tests; (a) characteristic strength, σ_0, (b) Weibull exponent *m* (widths and heights of rectangles given by the 90% confidence intervals).

4 DISCUSSION

In the experiments, we found

- a linear relation between the Weibull parameters, σ_0, for the bending strength and the contact strength with roughly $\sigma_{0,bend} \approx \sigma_{0,contact}$,
- and lower Weibull exponents in the roller tests compared to the 4-point bending tests.

A possible explanation of the very different Weibull exponents may be based on the pronounced stress gradients near the contact region. This calls for an evaluation of single cracks. In contrast to this query, the bending tests exhibit uniaxial stress states and negligible stress gradients.

The fracture mechanics background of the Weibull distribution under moderate stress gradients is based on the stress intensity factor, K,

$$K = \sigma * Y\sqrt{a} \tag{8}$$

with Y as a constant. This assumption is always fulfilled for bending tests, but violated in a contact strength test near the loading cylinders.

The relevant stress components, σ_x and τ_{xy}, are plotted over the cross-section of the bar in Fig. 2. In order to allow the stress intensity factors to be determined simply from the stresses, the natural cracks are modelled here as edge cracks.

From the stresses present in the uncracked body, the stress intensity factors, K_I and K_{II}, can be computed according to

$$K_I = \int_0^a h_I(\eta, a)\,\sigma_x(\eta)\,d\eta \quad , \quad K_{II} = \int_0^a h_{II}(\eta, a)\,\tau_{xy}(\eta)\,d\eta \tag{9}$$

with the weight functions h_I for mode-I and h_{II} for mode-II loading and the distance, η, from the surface.

The results are plotted in Fig. 4a and 4b. It is obvious from this representation that the mode-I stress intensity factors are first positive due to the tensile stresses near the free surface, ($y/H \rightarrow 1$ in Fig. 2a), and then become negative at greater depths. In this case, at least partial crack closure must occur. The remaining stress intensity factor, K_{II}, is reduced by crack surface friction.

The effective stress intensity factor, K_{eff}, combining K_I and K_{II}, was computed by [5]

$$K_{eff} = \begin{cases} \sqrt{K_I^2 + K_{II}^2} & \text{for} \quad K_I > 0 \\ K_{II} + \mu K_I & \text{for} \quad K_I < 0 \end{cases} \tag{10}$$

The coefficient, μ, was chosen as $\mu = 0.5$.

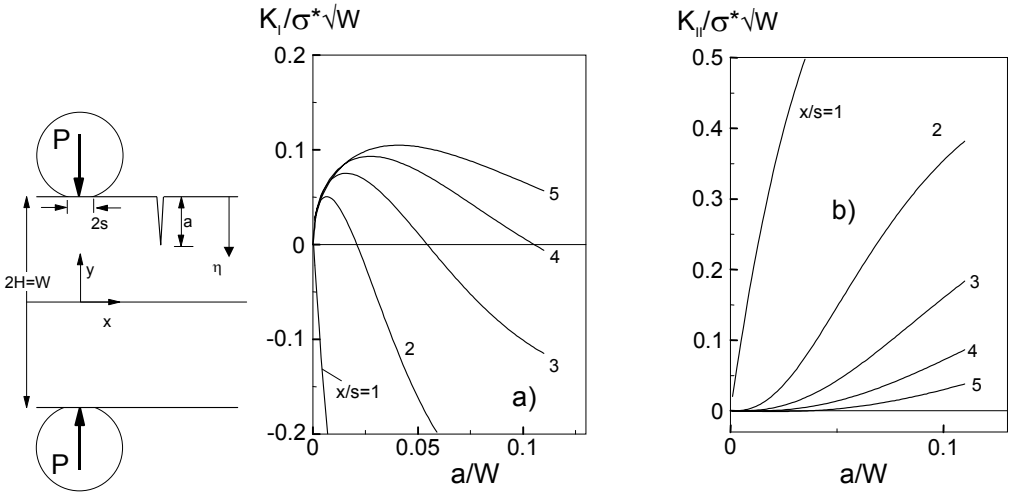

Fig. 5 Stress intensity factors for edge cracks, (a) mode-I and (b) mode-II stress intensity factor, ($s/H = 0.1$).

In Fig. 6a, the effective stress intensity factor, K_{eff}, is plotted versus the distance, x, from the contact centre for several crack depths, a. Maximum stress intensity factor values are visible near the location x/s=1, i.e. directly at the end of the Hertzian contact. For very small natural cracks of the kind present in high-strength ceramics, ($a/W \approx 0.01$ or smaller), failure must also be expected to occur at some distance from the Hertzian contact, i.e. near $x/s \approx 2$-4.

From this representation, it must be expected that specimens under contact loading predominantly fail near $x/s = 1$. This is in agreement with the experimental observation.

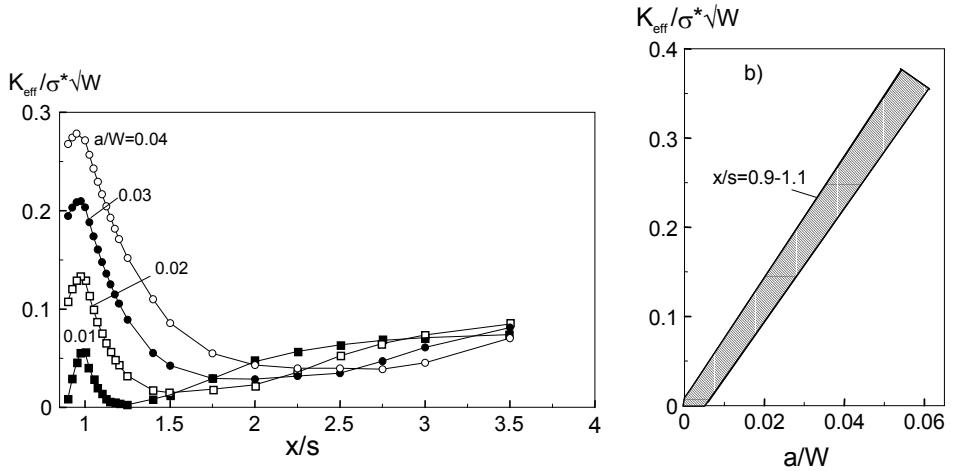

Fig. 6 (a) Effective stress intensity factor, K_{eff}, edge cracks of various depths as a function of the distance, x, from the contact centre, (b) effective stress intensity factors near the end of the Hertzian contact ($x/s \approx 1$).

In Fig. 6b, the effective stress intensity factor is plotted versus the relative crack depth, a/W, for locations near $x/s = 1$. It can be concluded from this representation that the effective stress intensity factor does not obey the usual proportionality of $K \propto \sqrt{a}$ near the Hertzian contact. In a rough description, the results may be expressed by a straight line,

$$K_{eff} \cong 6\sigma^* \sqrt{W}\,\frac{a}{W} \tag{11}$$

as indicated by the dash-dotted line in Fig. 9b.

The distribution functions, $F(a)$, of the crack size, a, of the most serious crack and of the strength, $F(\sigma_c)$, are related by (see, e.g., [6])

$$F(\sigma_c) = 1 - \exp[-zS(1 - F(a))] \ , \tag{12}$$

where z is the crack density (the number of cracks per surface unit) and S the surface of the component. The asymptotic behaviour of the flaw size distribution can be described by a power law,

$$f(a) \propto \frac{1}{a^r} \ , \tag{13}$$

from which the crack distribution function results as

$$F(a) = 1 - \left(\frac{a_0}{a}\right)^{r-1} \text{ for } a > a_0 \ . \tag{14}$$

Consequently, the strength distribution, $F(\sigma_c)$, reads

$$F(\sigma_c) = 1 - \exp\left[-zS\left(\frac{a_0}{a}\right)^{r-1}\right] \ . \tag{15}$$

Any specific value of crack size, a, has a corresponding value of σ_c. Introducing the relation between crack size and strength results in

$$a = \left(\frac{K_{Ic}}{Y\sigma_c}\right)^2 \Rightarrow F(\sigma_c) = 1 - \exp\left[-\left(\frac{\sigma_c}{\sigma_0}\right)^m\right] \tag{16}$$

This is a Weibull distribution with the parameters

$$m = 2(r-1) \ , \quad \sigma_0 = \frac{K_{Ic}}{Y\sqrt{a_0}\,(zS)^{1/m}} \ . \tag{17}$$

In the *contact loading test*, we find for the condition of the critical effective stress intensity factor equalling the mode-II fracture toughness, K_{IIc},

$$a = K_{IIc}\sqrt{W}\,/\,6\sigma^* \tag{18}$$

or if we replace σ^* by the maximum tensile stress according to (5), with $\sigma_{max} = 0.49\,\sigma^*$ interpreted as the contact strength, σ_c,

$$a = \lambda(s/H, \mu)\,\frac{K_{IIc}\sqrt{W}}{\sigma_c}, \quad \lambda = 0.082 \ \text{ for } s/H = 0.1, \mu = 0.5 \qquad (19)$$

Introducing this into (15) yields the following Weibull exponent under contact loading:

$$m_{\text{contact}} = r - 1 = \tfrac{1}{2} m \ . \qquad (20)$$

This is in complete agreement with the experimental data. For failure-relevant cracks in the range of approx. 40-100 μm and a specimen width of $W = 3$ mm, the result is $\sigma_{c,contact}/\sigma_{c,bend} \approx 0.9\text{-}1.4$, as estimated in [5].

SUMMARY

Strength tests of ceramic bars were performed under opposed cylinder loads. As examples of application, strength measurements were carried out of two aluminum oxides. From these results and former tests of HPSN and AlN it was found that the Weibull parameter, *m*, for the contact strength tests is about half that for bending tests. This can be explained by the pronounced stress gradients in the contact strength test. Application of the weight function method allowed the relation between the mixed-mode stress intensity factor and the crack length to be calculated. The effective stress intensity factor was found to be approximately proportional to the crack length. This leads to the reduced Weibull parameter, compared to the bending test.

Acknowledgement: The authors would like to thank the Deutsche Forschungsgemeinschaft DFG for financing this work within the SFB 483.

REFERENCES

[1] Fett, T., Munz, D., Thun, G. (2001), *Journal of Testing and Evaluation* **29**, 1.
[2] Thoman, D.R., Bain, L.J., Antle, C.E. (1969) *Technometrics* **11**, 445.
[3] European Standard ENV 843-5, Advanced monolithic ceramics - mechanical tests at room temperature - statistical analysis, European Committee for Standardisation, CEN TC184/WG3, London, UK.
[4] Badenheim, D., Oberacker, R. (2002), in: Proceedings of "Statuskolloquium Sonderforschungsbereich 483", Karlsruhe, 22.01.2002, 63-74.
[5] Fett, T., Munz, D. (1999) Influence of stress gradients on failure in contact strength tests with cylinder loading, to be published in *Engineering. Fracture Mechanics*.
[6] Munz, D., Fett, T. (1999) *CERAMICS Failure, Material Selection, Design*, Springer-Verlag, Heidelberg